First Measurement of the Giant Monopole and Quadrupole Resonances in a Short-Lived Nucleus: ^{56}Ni

C. Monrozeau,[1] E. Khan,[1] Y. Blumenfeld,[1] C. E. Demonchy,[2] W. Mittig,[3] P. Roussel-Chomaz,[3] D. Beaumel,[1] M. Caamaño,[4] D. Cortina-Gil,[4] J. P. Ebran,[1] N. Frascaria,[1] U. Garg,[5] M. Gelin,[3] A. Gillibert,[6] D. Gupta,[1,*] N. Keeley,[6] F. Maréchal,[1] A. Obertelli,[6] and J-A. Scarpaci[1]

[1]*Institut de Physique Nucléaire IN2P3/CNRS, Université Paris Sud, 91406 Orsay Cedex, France*
[2]*Department of Physics, Olivier Lodge Laboratory, University of Liverpool, Liverpool L69 7ZE, United Kingdom*
[3]*GANIL, DSM/CEA, IN2P3/CNRS, BP 5027, 14076 Caen Cedex 5, France*
[4]*Universidad Santiago de Compostela, E-15706 Santiago de Compostela, Spain*
[5]*Physics Department, University of Notre Dame, Notre Dame, Indiana 46556, USA*
[6]*CEA/DSM/DAPNIA/SPhN, Saclay, 91191 Gif-sur-Yvette Cedex, France*

(Received 19 July 2007; published 28 January 2008)

The isoscalar giant monopole resonance (GMR) and giant quadrupole resonance (GQR) have been measured in the ^{56}Ni unstable nucleus by inducing the ^{56}Ni(d, d') reaction at 50A MeV in the Maya active target at the GANIL facility. The GMR and GQR centroids are measured at 19.3 ± 0.5 MeV and 16.2 ± 0.5 MeV, respectively. The corresponding angular distributions are extracted from 3° to 7°. A multipole decomposition analysis using distorted wave Born approximation with random phase approximation transition densities shows that both the GMR and the GQR exhaust a large fraction of the energy-weighted sum rule. The demonstration of this new method opens a broad range of giant resonance studies at intermediate-energy radioactive beam facilities.

DOI: 10.1103/PhysRevLett.100.042501 PACS numbers: 24.30.Cz, 21.10.Re, 24.50.+g, 27.40.+z

Over the past few years the focus of nuclear structure has moved toward short-lived exotic nuclei. Major discoveries of unexpected new phenomena have been recorded, such as neutron haloes and skins [1] and the modification of magic numbers far from stability [2]. Giant resonances are collective excitations of nuclei involving a large fraction of the constituent nucleons. They have proved to be a major source of information on collective and single-particle properties of atomic nuclei [3]. The reproduction of their properties represents a strong constraint for nuclear models, in particular, modern microscopic approaches based on the density functional theory [4]. Fundamental nuclear properties such as the equation of state of nuclear matter or the effective nucleon-nucleon interaction have benefited from detailed measurements of giant resonances (GR's) [5]. The study of GR's in exotic nuclei is thus expected to enhance our understanding of exotic nuclear structure. Experimentally such studies encounter major hurdles and have until now been limited to the isovector giant dipole resonance in neutron-rich oxygen [6], neon [7] and tin isotopes [8]. They provided the first evidence for soft E1 modes in unstable nuclei.

The isoscalar giant monopole resonance (GMR) is of major importance because its properties are related to the nuclear matter incompressibility K_∞. The interest in determining K_∞ stems from its impact on the nuclear matter equation of state. Some significant progress in our understanding of how K_∞ can be constrained has been achieved in recent times. Namely, the procedure generally adopted to extract the incompressibility from the measurement of the GMR energy [9] is based on energy functionals that allow one to calculate finite nuclei and nuclear matter on the same footing [10]. The first step consists in constraining the energy functional in order to reproduce the experimental value of the monopole energy in a given nucleus [11,12]. Then using this constrained energy functional, the value of K_∞ is extracted.

Within the relativistic and nonrelativistic frameworks, K_∞ can be fixed with an accuracy of $\sim$10% [12]: $K_\infty \approx$ 230–250 MeV. Part of the uncertainty is due to our poor knowledge of the symmetry energy [12]. Therefore, the investigation of the GMR along isotopic chains should be relevant to probe the role played by the symmetry energy in the determination of the nuclear matter incompressibility. Moreover, the incompressibility of asymmetric matter is a basic parameter in calculations describing neutron stars or supernovae [13]. Measurement of the GMR in neutron-rich systems may be a milestone toward testing the energy functionals to predict the equation of state in asymmetric infinite matter.

It is therefore tantalizing to achieve a pioneering method to measure the GMR in unstable nuclei. The ^{56}Ni nucleus plays a major role in stellar nucleosynthesis: it was observed in the ejecta from supernova 1987A [14] and is related to the so-called iron peak. This provides strong motivation to investigate the structure of this nucleus, as stressed in Ref. [15]. The measurement of GMR and giant quadrupole resonance (GQR) in ^{56}Ni also represents a first step in the study along the Ni isotopic chain.

The best probes for the investigation of the GMR and the GQR are isoscalar probes such as deuterons or α particles at energies between a few tens and a few hundreds A MeV

[3]. No such experiment has been performed for unstable nuclei up to now, due to the difficult conditions in reverse kinematics. Indeed, the GMR cross section peaks at 0° in the center of mass frame, which gives rise to very low recoil velocities for the light probe. To measure the excitation energy range between 0 to 30 MeV in reverse kinematics, it is necessary to detect the recoiling particle (d or α) with energies ranging from 100 keV to 2 MeV at angles from 0 to 40° in the laboratory frame. A standard setup with a recoiling particle telescope would necessitate a very thin target ($\sim 100\ \mu g/cm^2$) to minimize straggling and thus require an intensity of over 10^7 pps, which is prohibitive for current radioactive beam facilities.

With respect to the above experimental constraints, an active target such as Maya [16] is the key to measuring the GMR and GQR in unstable nuclei. In an active target, the detector gas also acts as target. Such a setup has, in principle, an angular coverage close to 4π, a low energy threshold and a large effective target thickness. In this Letter we report on the first measurement of the GMR and the GQR with a radioactive beam using this new experimental technique.

In the domain of secondary beams, the active target archetype is the detector IKAR [17] which was used at the GSI facility. The Maya target, developed at GANIL for the lower-energy domain [16], can be characterized as a $28 \times 26 \times 20\ cm^3$ time and charge projection chamber. The electrons from the ionization of the gas by particles drift down the electric field to amplifying wires set parallel to the beam. For a two-body reaction, scattered and recoiling particles are in a plane that can be determined by the drift time to the wires. The amplified signal is induced on the anode, a matrix of 35×34 pads connected to Gassiplex [18] chips. A hexagonal structure was chosen for these pads in order to have the best conditions for the reconstruction of the projected recoil trajectory, independent of the recoil direction.

The secondary ^{56}Ni beam at 50A MeV ($\pm 0.5\%$ energy spread) was produced at the GANIL facility by fragmentation of ^{58}Ni at 75A MeV on a 70.5 mg/cm^2 C target located in the SISSI [19] device and purified by passing through a 135 mg/cm^2 Al degrader placed between the two dipoles of the Alpha fragment separator before being sent to the SPEG area. The Maya target was placed on the focal plane of the SPEG spectrometer [20], which was used to purify the beam, so only $^{56}Ni^{27+}$ was transmitted. Two plates were added above and below the beam trajectory in the Maya target to prevent the highly ionizing beam particles from inducing charges. However, due to the angular spread of the beam, some noninteracting ^{56}Ni ions were detected. This limited the beam intensity that could be used to 5×10^4 pps, while 10^6 pps of ^{56}Ni were available.

The Maya active target was filled with deuterium gas, at a pressure of 1050 mbar, forming a pure deuterium target of 1.6 mg/cm^2 (equivalent to a target of 6.3 mg/cm^2 of CD_2). It should be noted that α-particle scattering, which would be the preferred probe for the GMR, could not be undertaken because the detector, like any gaseous detector, sparked when filled with pure He. As pointed out above, reverse kinematics generate recoil particles in a large energy domain. High energy light particles such as deuterons with $E \geq 2$ MeV were not stopped in the Maya gas volume. For such escaping particles, we added ancillary 500 μm Si detectors outside the active volume covering from 10 to 60 degrees around the beam direction for events occurring at the center of the detector. For normalization purposes the beam was counted in a polycrystalline diamond detector of 1 cm^2 surface and 100 μm thickness, after traversing the Maya target.

For each event two physical observables are determined in order to reconstruct the kinematics of the reaction: the energy and the angle of the recoil. The recoiling angle in the horizontal plane is reconstructed by a linear least squares fit of the positions of the pads hit with a weight proportional to the amount of charge deposited. In order to obtain a reliable trajectory, at least 10 pads with nonzero charges were required corresponding to 5 cm long trajectories, which introduced an effective deuteron threshold of 700 keV. The reaction plane is determined from the drift times of the electrons toward the anode wires. The inter-

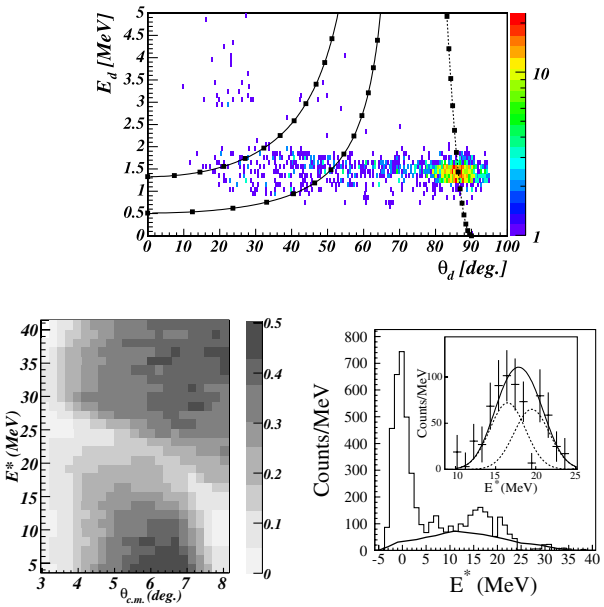

FIG. 1 (color online). Top: Scatter plot of recoiling deuteron energy versus scattering angle in the laboratory frame for the ^{56}Ni beam. The lines correspond to elastic scattering and the 14–22 MeV excitation energy of ^{56}Ni. The c.m. angles ares denoted by squares along these lines, with 1° step, starting from 0° for the lowest deuteron energy. Bottom left: geometrical efficiency of the detection setup in the c.m. frame. Bottom right: ^{56}Ni excitation energy spectrum deduced from the deuteron kinematics and corrected for geometrical efficiency. The background that was subtracted is shown by the solid line. The inset shows the background subtracted inelastic data fitted with Gaussian distributions located at 16.5 and 19.5 MeV for the GQR and the GMR, respectively, (see text).

section of the deuteron trajectory with the beam axis gives the vertex of the interaction. The recoil stopping point is determined by projecting the charges on the direction of the trajectory whose maximum corresponds to the Bragg peak. For each event, the recoil angle and the range in the deuterium gas are therefore determined. The energy of the recoil is then deduced from its range in the gas through energy-loss tables [21]. The 3D reconstruction of scattering trajectories in Maya provides the kinematics of the ^{56}Ni(d, d') reaction, shown in Fig. 1. The decrease of intensity to small recoiling deuteron angles is mainly due to the shielding of the beam, leading to an acceptance cut.

The data are then transformed into the center of mass frame using two-body relativistic kinematics. The corresponding excitation energy spectrum of ^{56}Ni corrected for the geometrical efficiency of the detector, is shown in Fig. 1. This spectrum presents a peak centered at 0 MeV corresponding to elastic and inelastic scattering towards low-lying states. It must be noted that, due to the accessible deuteron energy range, the elastic scattering is measured over only a very small angular domain in the center of mass frame, precluding the extraction of the corresponding angular distribution. For the elastic peak the FWHM is 3 MeV and is mainly induced by the trajectory reconstruction uncertainties, especially the vertex localization due to the beam shielding. At energies ranging from 12 to 25 MeV a bump in the excitation energy spectrum points to the presence of isoscalar giant resonances. Only deuterons corresponding to excitation energy below 25 MeV are stopped in the Maya detector, whereas the Si detectors placed 70 mm behind the Maya detector allow the energy spectrum between 28 and 35 MeV to be measured.

Since the pressure and the bias used in the experiment were optimized to detect very low deuteron energies, it was not possible to separate protons from deuterons through range versus charge measurements [16]. Consequently some proton contamination may be expected in the data. Protons can be produced essentially by two mechanisms: deuteron breakup and one neutron transfer (d, p) reactions. The latter will not be considered since the lowest energy protons are scattered at backward angles. The contribution of the deuteron breakup was estimated from direct kinematic measurements for ^{58}Ni at 50A MeV at larger angles ($\theta_{\mathrm{c.m.}} > 8°$) [22]. These data are extrapolated to lower angles and transformed to the reverse kinematics frame, corrected for the geometrical acceptance of the Maya detector, and normalized to the experimental data (Fig. 1). The shape of the deuteron breakup does not exhibit any bump in the giant resonance region but rather corresponds to a smooth background.

In order to extract the GMR and GQR centroid location and the corresponding angular distributions, a multipole decomposition analysis (MDA) is performed [3]. After subtraction of the background, experimental angular distributions were extracted for five excitation energy intervals and fitted by a linear combination of theoretical distributions for $L = 0$ and $L = 2$ excitations. The theoretical angular distributions are calculated using the distorted wave Born approximation (DWBA). Both real and imaginary optical potentials are microscopically determined using ^{56}Ni and deuteron densities within the double folding model with the Michigan three-range Yukawa (M3Y) interaction as in Ref. [23]. The deuteron density is obtained from the Hulthen deuteron wave function [24]. The ^{56}Ni nucleus densities are calculated with the Hartree-Fock model and the Sagawa Giai II (SGII) ($K_\infty = 217$ MeV) [5] Skyrme functional without including pairing since it is a doubly magic nucleus. The corresponding $L = 0$ and $L = 2$ strength functions are well concentrated, similar to those of Fig. 3 and 28, respectively, of Ref. [25]. No data are available for deuteron elastic scattering from the unstable ^{56}Ni nucleus; therefore the optical potentials are renormalized in order to reproduce ^{58}Ni(d, d) at 120 MeV [26]: the real part of the optical potential is increased by 7%. The GMR and GQR transition potentials are calculated with the same procedure, using microscopic RPA transition densities [27] obtained self-consistently from the same Skyrme functional as in the HF calculation. It should be noted that it is the first time that the GMR is measured for such a light nucleus using the (d, d') reaction.

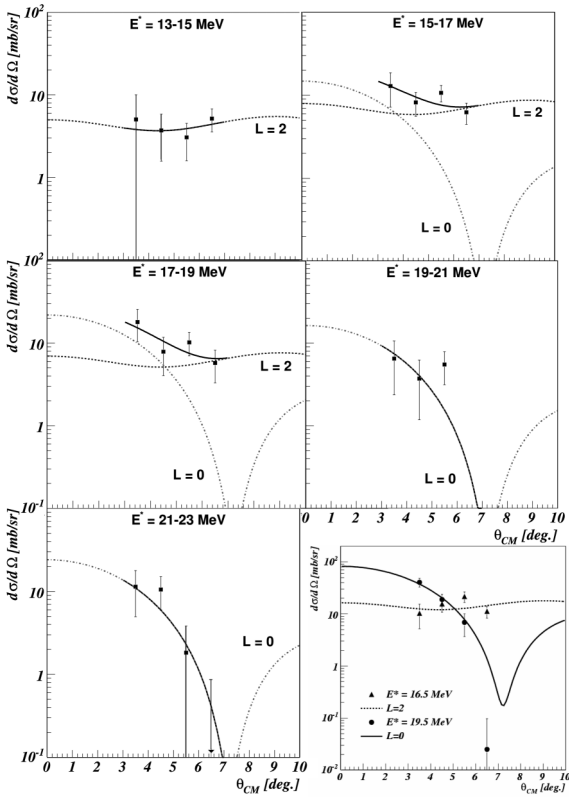

FIG. 2. GMR and GQR inelastic angular distributions of ^{56}Ni at 50A MeV and DWBA calculations using microscopic double folded RPA form factor (see text). The data (squares) are also displayed. Bottom right: analysis of the data obtained by using two Gaussian distributions located at 16.5 and 19.5 MeV for the GQR and the GMR, respectively, with FWHM = 5.2 MeV (see text).

TABLE I. GMR and GQR centroids and EWSR measured in ^{56}Ni, ^{58}Ni and ^{56}Fe.

	GMR		GQR	
	E_c (MeV)	% EWSR	E_c (MeV)	% EWSR
^{56}Ni	19.3 ± 0.5	136 ± 27	16.2 ± 0.5	76 ± 13
^{58}Ni [28]	$19.20^{+0.44}_{-0.19}$	85^{+13}_{-10}	$16.31^{+0.17}_{-0.10}$	82 ± 10
^{58}Ni [29]	$19.9^{+0.7}_{-0.8}$	92^{+4}_{-3}	$16.3^{+0.8}_{-0.9}$	73 ± 3
^{56}Fe [28]	$18.35^{+0.33}_{-0.19}$	98^{+14}_{-10}	$16.35^{+0.19}_{-0.10}$	77 ± 10

Consequently, the validity of reaction models cannot be thoroughly tested on stable nuclei for this reaction.

Figure 2 shows the angular distributions whose shapes are well reproduced by the calculations. As expected, the $L = 2$ mode dominates below 17 MeV, whereas the $L = 0$ mode is the largest above 17 MeV. The percentage of the exhausted energy-weighted sum rule (EWSR) is determined for each energy interval for both multipolarities. It is then straightforward to obtain the centroid of the giant resonances and the total exhausted EWSR (Table I). Error bars are purely statistical and do not take into account uncertainties on the background or on the reaction models. In order to cross-check the results, another independent analysis of the data was undertaken by fitting the excitation energy spectrum with the background shape and two Gaussian distributions corresponding to the GMR and the GQR, for different angles between 3° and 7°. The angular distributions of the Gaussian shapes are shown in the bottom right part of Fig. 2 and are well reproduced by DWBA calculations. The percentage of EWSR extracted by normalization are in close agreement with the MDA results.

The ^{56}Ni results are comparable to those obtained on ^{58}Ni and ^{56}Fe with (α, α') scattering [28,29] (Table I). The FWHM obtained by the Gaussian fits on the ^{56}Ni data (5.2 ± 0.5 MeV both for the GMR and the GQR) are also consistent with neighboring stable nuclei where FWHM between 5.5 and 7.7 MeV are found [28].

With only 15 h of effective data taking and an average beam intensity of 5×10^4 pps, isoscalar GMR and GQR resonances were measured in the ^{56}Ni unstable nucleus. It is the first measurement of these resonances in a short-lived nucleus. This makes the method relevant with respect to predicted production rates of a large domain of exotic nuclei at current and future facilities. A redesign of the detector in order to increase the amplification gain would allow access to smaller angle measurements and improve particle identification. Measurements in neutron-rich nickel isotopes up to ^{68}Ni could be undertaken now in order to probe the evolution of giant resonances along an isotopic chain. Also, measurements on heavier nuclei such as ^{132}Sn would complement the systematics already existing for stable tin isotopes [30].

This work has been supported in part by CNRS/IN2P3, CEA/DAPNIA and by the U.S. National Science Foundation (Grant No. PHY04-57120).

*Present address: Variable Energy Cyclotron Centre, 1/AF Bidhan Nagar, Kolkata 700064, India

[1] A. S. Jensen, K. Riisager, and D. V. Fedorov, Rev. Mod. Phys. **76**, 215 (2004).
[2] T. Otsuka T. Matsuo, and D. Abe, Phys. Rev. Lett. **97**, 162501 (2006).
[3] M. Harakeh and A. Van der Woude, *Giant Resonances* (Oxford University Press, New York, 2001).
[4] W. Kohn, Rev. Mod. Phys. **71**, 1253 (1999).
[5] Nguyen Van Giai and H. Sagawa, Nucl. Phys. A **371**, 1 (1981).
[6] A. Leistenschneider *et al.*, Phys. Rev. Lett. **86**, 5442 (2001).
[7] J. Gibelin *et al.*, Nucl. Phys. A **788**, 153c (2007).
[8] P. Adrich *et al.*, Phys. Rev. Lett. **95**, 132501 (2005).
[9] D. H. Youngblood *et al.*, Phys. Rev. Lett. **39**, 1188 (1977).
[10] J. P. Blaizot, Phys. Rep. **64**, 171 (1980).
[11] O. Bohigas, A. M. Lane, and J. Martorell, Phys. Rep. **51**, 267 (1979).
[12] G. Colò *et al.*, Phys. Rev. C **70**, 024307 (2004)
[13] N. K. Glendenning, *Compact Stars* (Springer-Verlag, New York, 1997).
[14] H. A. Bethe, Rev. Mod. Phys. **62**, 801 (1990).
[15] G. Kraus *et al.*, Phys. Rev. Lett. **73**, 1773 (1994).
[16] C. E. Demonchy *et al.*, Nucl. Instrum. Methods Phys. Res., Sect. A **573**, 145 (2007).
[17] A. A. Vorobyov *et al.*, Nucl. Instrum. Methods **119**, 509 (1974); Nucl. Instrum. Methods Phys. Res., Sect. A **270**, 419 (1988).
[18] J. C. Santiard *et al.*, CERN Report No. CERN-ECP-94-17, 1994.
[19] R. Anne, Nucl. Instrum. Methods Phys. Res., Sect. B **126**, 279 (1997).
[20] L. Bianchi *et al.*, Nucl. Instrum. Methods Phys. Res., Sect. A **276**, 509 (1989).
[21] L. C. Northcliffe and R. F. Schilling, Nucl. Data Sect. A **7**, 233 (1970).
[22] D. Ridikas *et al.*, Phys. Rev. C **63**, 014610 (2000).
[23] J. Cook, Nucl. Phys. A **382**, 61 (1982).
[24] L. Hulthén and M. Sugarawa, *The Two-Nucleons Problem* (Springer-Verlag, Berlin, 1957).
[25] J. Terasaki and J. Engel, Phys. Rev. C **74**, 044301 (2006).
[26] A. C. Betker *et al.*, Phys. Rev. C **48**, 2085 (1993).
[27] P. Chomaz *et al.*, Phys. Lett. B **281**, 6 (1992).
[28] Y.-W. Lui *et al.*, Phys. Rev. C **73**, 014314 (2006).
[29] B. K. Nayak *et al.*, Phys. Lett. B **637**, 43 (2006).
[30] T. Li *et al.*, Phys. Rev. Lett. **99**, 162503 (2007).